

Relationships Between Meteorological Conditions and Cloud Properties Determined from ARM Data

Y.-H. Yi

*Analytical Services and Materials, Inc.
Hampton, Virginia*

P. Minnis

*National Aeronautics and Space Administration (NASA)
Hampton, Virginia*

*J. K. Ayers, J.-P. Huang, D. R. Doelling, M. M. Khaiyer, and M. L. Nordeen
Analytical Services and Materials, Inc.
Hampton, Virginia*

Introduction

Improvements of cloud model parameterizations require basic knowledge of the relationships between measured and modeled meteorological state parameters and the cloud properties in a given volume of air. The uncertainty in the relationships, especially large for cirrus clouds, is exacerbated by the differences between actual soundings and those produced by analyses.

The cloud vertical structure, including top and base heights, layer thickness, and the characteristics of multilayered clouds, has been examined by Wang et al. (1995) by using radiosonde data. Cloudy layers are identified by relative humidity (RH) values above a threshold value of 84%. Cloud-layer top and base are identified by sudden changes in RH. These changes are positive at the base and negative at the top. The use of a constant threshold value for RH might misclassify clear moist layers as cloudy layers in boundary layer, and drier cloudy layers as clear layers in middle to upper troposphere. With the availability of the Active Remotely Sensed Cloud Location (ARSCL) (Clothiaux et al. 2001) cloud product at the Atmospheric Radiation Measurement (Program) Southern Great Plains (ARM SGP) central facility site, the RH threshold values changing with temperature can be examined.

Routine surface cloud observations see only the lowermost cloud layer in a column while the satellites see only the uppermost cloud layer. With the availability of high temporal and spatial resolution analyses and satellite cloud retrievals, it is imperative to better understand the relationships between measured and modeled meteorological state parameters and the cloud properties in a given volume of air.

Cloud-free ice-supersaturated (with respect to ice) air masses have been detected by various types of observations. Such regions have been termed “ice-supersaturated regions” (ISSRs) (Gierens et al. 1999). A good marker of ISSR is persistent condensation trails (contrails) when the sky is otherwise free of clouds. The formation and persistence of contrails do not require as high ambient humidity as

the formation of natural cirrus (Minnis et al. 2004). Spichtinger et al. (2003) used carefully calibrated and corrected RS80-A radiosondes to detect ice supersaturation. Unfortunately, radiosonde reports do not contain any information about the concentration of ice crystals along their path; therefore, it is not possible to distinguish between cloudy and cloud-free parts of the profile. With the ARSCL cloud product at ARM SGP central facility (CF), it is possible to detect cloud-free ice-supersaturation layers.

In this study, the differences between RH and temperature values are examined using both reanalysis data and radiosonde atmospheric profiles obtained at the ARM SGP. The probabilities of detecting clouds estimated as functions of RH and temperature. From these estimates, a temperature-dependent RH threshold function is developed for different probabilities. Finally, the occurrence of cloud-free ice-supersaturation layers in the upper troposphere is investigated by utilizing Rapid Update Cycle (RUC) and radiosonde data and the statistical properties of RH in cloud-free supersaturated and subsaturated layers are studied.

Data

RUC Reanalysis Data

The modeled atmospheric profiles of height, temperature, RH, and horizontal and vertical wind speeds were derived from the 40-km resolution, 1-hourly (RUC40) analyses (Benjamin et al., 2004a and 2004b) in 25 hPa intervals from the surface to 100 hPa. The values at the RUC grid point closest to the SCF (36.617 °N, -97.5 °W) site were used in this study.

Radiosonde (SONDE) Data

Radiosonde (SONDE) data collected at the SCF from March 1, 2000 to February 28, 2001 were used as the best available atmospheric profiles. There are normally four radiosonde launches per day, at 00, 06, 12, and 18 UTC, respectively. During Intensive Operation Periods (IOPs), which typically occur 3 to 5 times per year, radiosondes are launched 8 times per day at the SCF. They provide high-resolution profiles of pressure, temperature, RH with respect to liquid water, and wind speed and direction. The reported values cover the pressure range from the surface to maximum observation level.

To reduce RH measurement noise and facilitate processing, the radiosonde profiles were vertically smoothed into 25 hPa interval profile from the surface to 100 hPa. The time of the sounding midpoint was determined for each radiosonde ascent and matched with the closest hourly RUC analysis profile. The RH from both SONDE and RUC data is defined with respect to liquid water at all temperature and is converted to RH with respect to ice (RHI) at temperatures less than or equal to 253°C K since liquid-phase clouds may exist at temperature as low as -39°C.

Cloud Boundary Data

The ARSCL cloud product consists of cloud base and top heights for each 10-second interval using the algorithms of Clothiaux et al. (2001) with a combination of Belfort Laser Ceilometer (BLC), Millimeter Wave Cloud Radar (MMCR), and Micropulse Lidar (MPL) data. The cloud base and top heights used in this study are 10-min averages centered on the RUC times.

Analysis and Results

The combined dataset consists of 1150 soundings matched with RUC profiles and ARSCL cloud boundary data. Using ARSCL cloud boundary data, each layer in the SONDE and RUC data can be identified as a cloud-free or cloud layer. If all layers are cloud-free for a given profile, then it is defined as a clear-sky sounding, otherwise, as a cloudy-sky sounding. About 60% of these soundings or RUC profiles are classified as clear-sky soundings with the remaining 40% classified as cloudy-sky soundings. Figure 1 shows the vertical distribution of cloudy and clear layer in cloudy-sky soundings. From the surface up to 100 hPa, the frequency of cloud layer occurrence is less than 14%. The maximum occurrences of cloud layers are in the upper (300 hPa) and lower (975 hPa) troposphere, respectively. The middle troposphere has relatively fewer occurrences of clouds. Above 300 hPa, the occurrence of cloud-free layers increases dramatically since the tropopause height varies between 100 and 300 hPa.

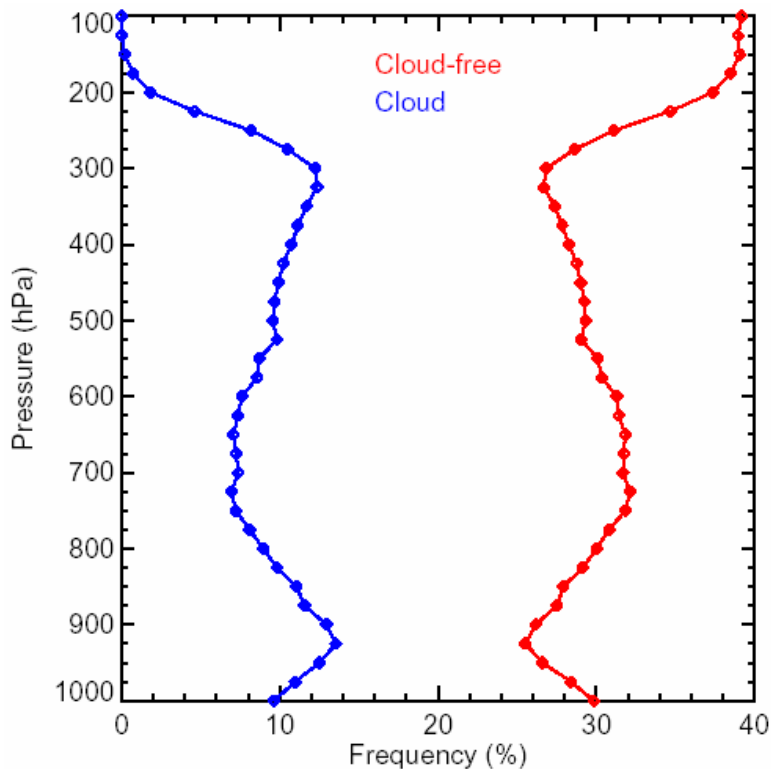


Figure 1. Vertical distribution of the frequency of cloudy and cloud-free layer in cloudy-sky soundings. The frequency of the clear sky cases examined was 60%, not shown here.

Comparison of SONDE and RUC

Relative humidity is a quantity that usually displays a very intricate structure in space and time. Since it depends on both absolute humidity and temperature, fluctuations of both these fields translate into RH fluctuations.

Figure 2 shows the comparison of hourly RUC (blue line) and SONDE (red line) atmospheric profiles at 21 UTC April 4, 2000 (left) and 12 UTC 3 November 2000 (right). The cloud layer location determined from the ARSCL cloud base and top height is illustrated by the gray area. As shown in the left figure, the RUC and SONDE profiles agree in regard to cloud location but differ significantly in RH outside the cloud layer. The RH values associated with this cloud layer are below ice saturation. The right figure shows that the SONDE accurately predicts cloud location but the RUC is very dry and provides no indication of cloud location. A cloud-free moist layer (RH >90%) exists around 10 km. The moist layer shown in the SONDE profile is broader (span from 7km to 12 km) than one in RUC. These differences may be due to smoothing of the fields by RUC.

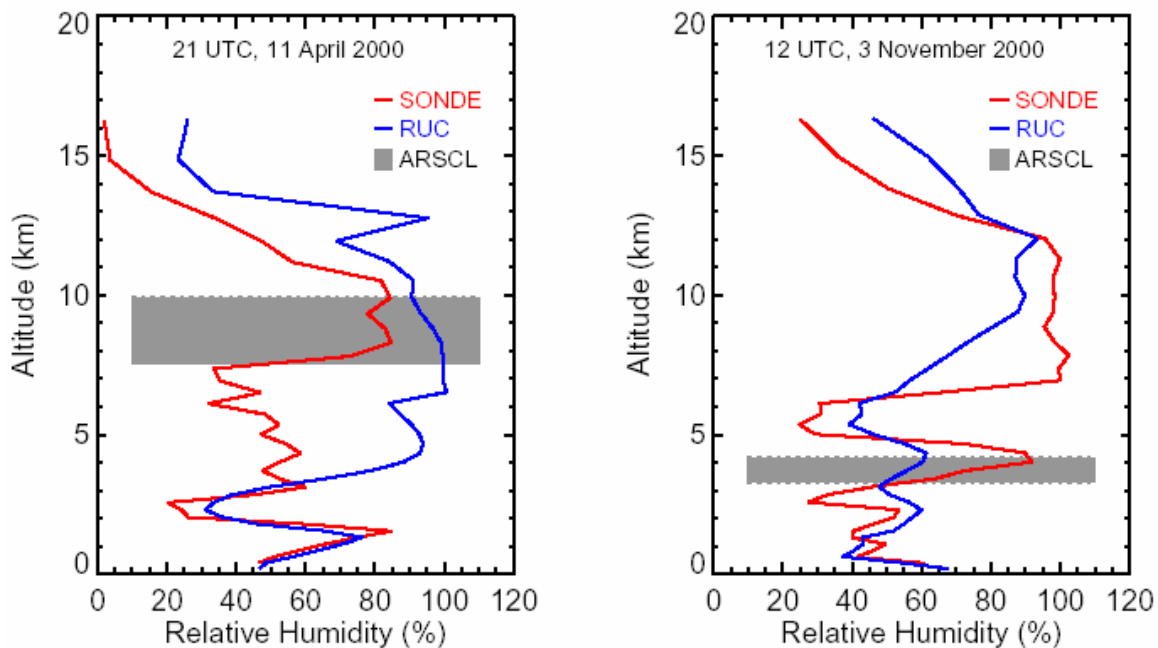


Figure 2. The RH profiles from SONDE (red solid line) and RUC (blue solid line) at 21 UTC on April 11, 2000 and at 12 UTC on November 3, 2000. The gray area represents cloud layers determined from ARSCL's cloud base and top heights.

Figure 3 shows scatterplots of the RH and temperature from SONDE and RUC data in the upper troposphere (250 - 350 hPa) inside clouds. The temperature observations from the SONDE and RUC are highly correlated. The RHs are somewhat correlated, but the SONDE values are generally greater than those from RUC. These results were expected since comparisons of matched SONDE and RUC tend to show that the RUC RH is lower than its radiosonde counterpart at higher values of RH. This bias may be due the RUC model constraining humidity values.

Some magnitude of differences in RH between RUC and SONDE data are expected since the RH profile actually represents the grid average of the RH field from RUC reanalyses, in which the humidity values above the tropopause have been constrained to saturation. However, the radiosonde, being a point measurement, reports the actual instrument-measured atmospheric thermodynamic state if the biases in RH due to instrument errors (Wang et al. 2002, Turner et al. 2003) are ignored. Thus, RUC may not reflect or capture some cloud information, especially for short term and small scale cloud systems.

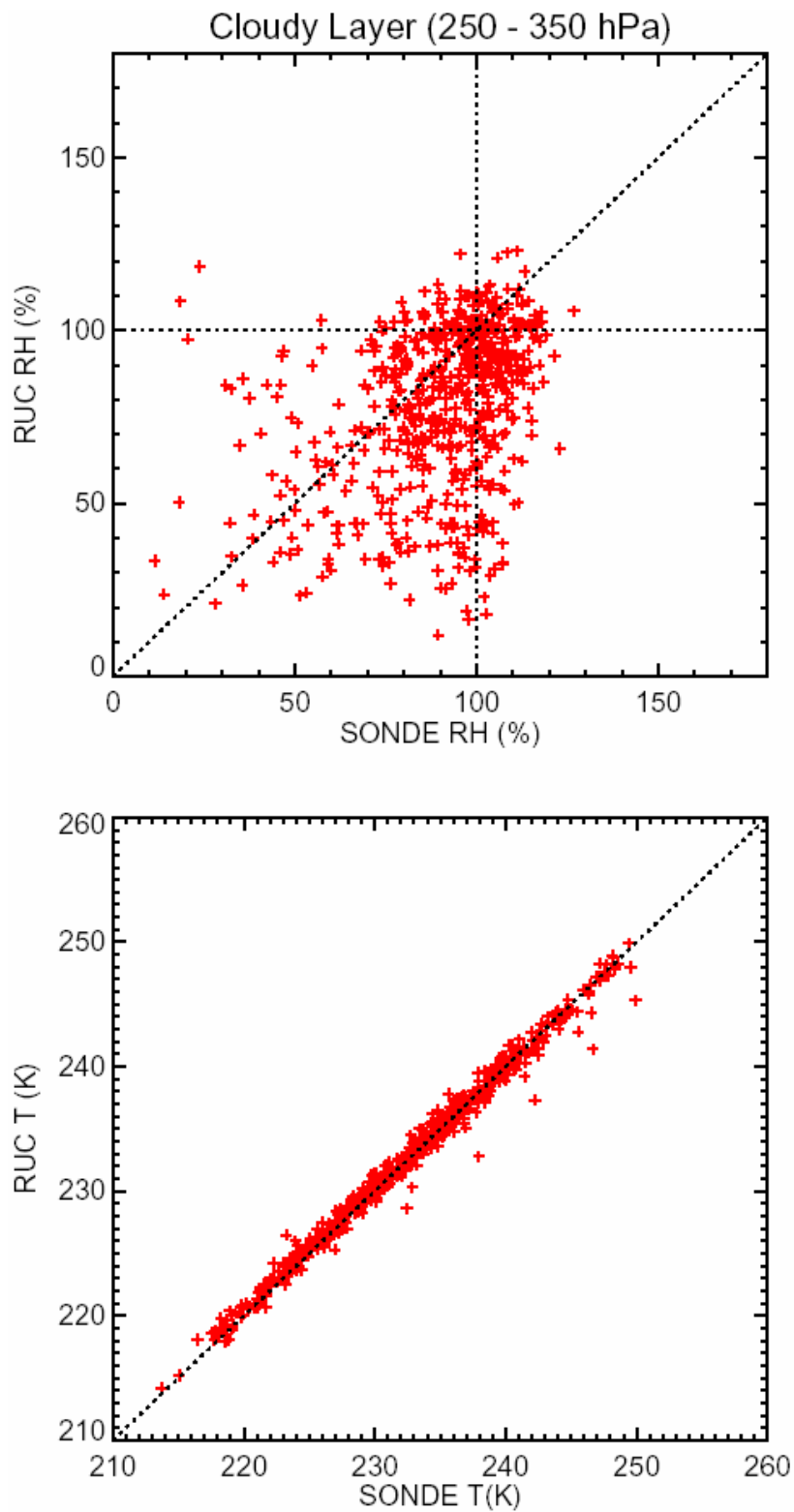


Figure 3. Scatterplot comparisons of the RH and temperature inside clouds from SONDE and RUC in the upper troposphere, 250 hPa to 350 hPa.

Histograms of from SONDE and RUC RH in clear and cloudy conditions are shown in Figure 4. For both datasets, the frequency distributions are distinctly different between clear and cloud conditions for all layers. The SONDE histograms are more peaked compared to the smoothed RUC data. The ice supersaturation layers exist inside clouds (solid blue steps on the right side of black vertical dotted line) and outside clouds (solid red and brown steps on the right side of black vertical dotted line) in the upper troposphere (100 hPa to 400 hPa). The large fluctuations in RH result in a heavy-tailed frequency distribution.

The vertical distributions of RH and T differences between SONDE and RUC data in clear and cloud conditions are shown in Figure 5. Inside clouds (blue curve), the RH from RUC is 2-14 % lower than the RH from SONDE for all RUC layers. There is no significant RH difference between SONDE and RUC data outside cloud (red curve) or in clear sky (brown curve) in the lower troposphere (below 500 hPa). Above 500 hPa, however, the RUC seems to be moister than the SONDE with the difference between SONDE and RUC increasing with height (decreasing pressure), especially in the upper troposphere.

The RUC model contains a sophisticated cloud and moisture scheme that allows for ice – supersaturation. As indicated by Figure 4, it does not compute enough supersaturation. This finding is consistent with the results of Duda et al. (2004) who demonstrated that the RUC underestimates upper tropospheric humidity by showing that persistent contrails developed in regions where the RUC40 computed an RHI of only 85%.

The variations of the SONDE and RUC layer mean RH with the layer mean temperature in clear and cloud conditions are shown in Figure 6. The impact of the arbitrary selection of $T = 253$ K for a switch from RH to RHI is evident in the minima in the curves around $T = 255 - 260$ K. Although the layer mean RH inside clouds is well separated from layer mean RH outside cloud or in the clear-sky, RH thresholds chosen as a function of temperature can more accurately diagnose cloud occurrence.

RH Thresholds in SONDE and RUC

In order to find the relationships between RH threshold and temperature, RH values are grouped according to the associated ambient temperature resulting in a frequency distribution for each temperature interval. Figure 7 shows the frequency distributions of RH when the ambient temperature is between 250 and 254 K. The histogram (solid blue steps) and Gaussian fit (blue dotted line) are presented together in the upper panel. The cumulative distribution functions in clear and cloud conditions are shown in the lower panel of Figure 7. The blue solid and dotted lines show that the histogram and Gaussian fit are in good agreement, which indicates that the RH inside clouds can be described by a Gaussian (normal) distribution. However, the RH outside cloud (red) and in the clear sky (brown) can not be represented by a normal distribution but might be represented better using an exponential distribution (see section d below). Ovarlez et al. (2002) also found that the RH statistics outside and inside of clouds are fundamentally different: the RH within clouds turns out to be better described by either a Gaussian or a Rayleigh distribution centered at saturation.

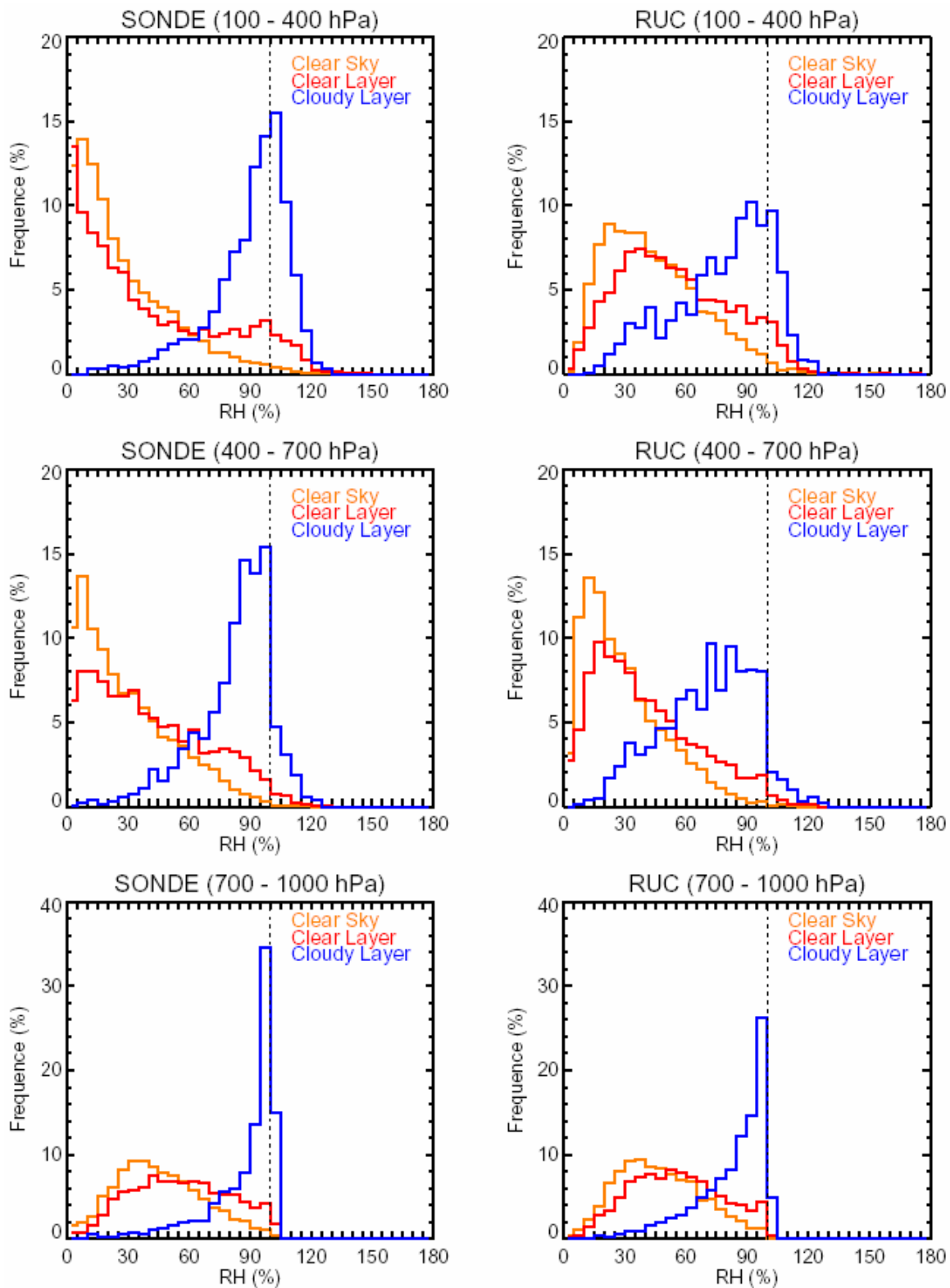


Figure 4. Histograms of the RH from SONDE and RUC in clear and cloud conditions.

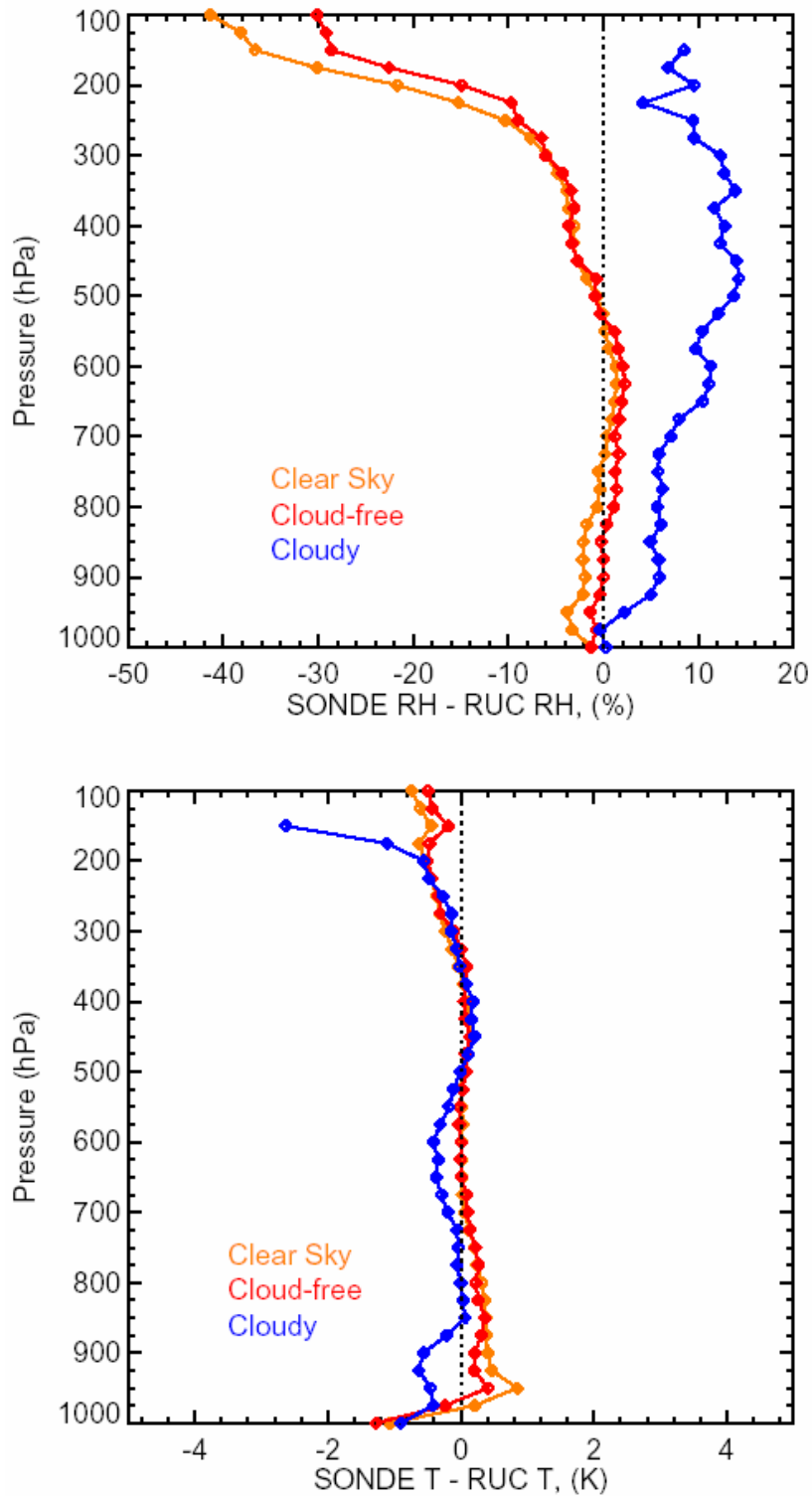


Figure 5. Vertical distribution of RH and T difference between SONDE and RUC in clear and cloud conditions.

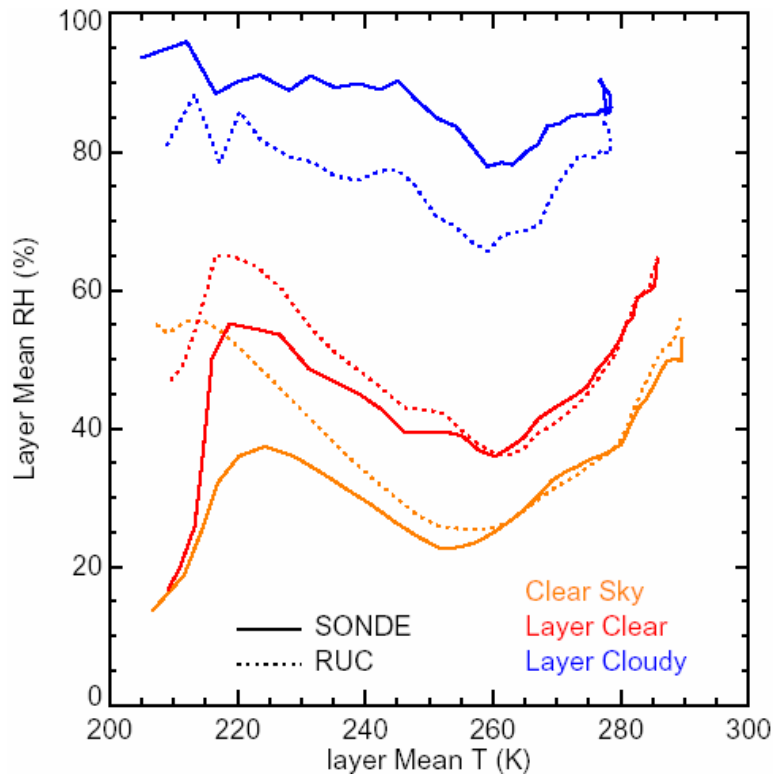


Figure 6. Variations of the SONDE and RUC layer mean RH with the layer mean temperature for clear and cloud conditions.

From the cumulative distribution functions (lower panels of Figure 7), it is shown that, when $RH < 67.52\%$ for SONDE and 48.37% for RUC, the probability of finding a cloud is 20%. Conversely, when the RH is greater than 67.52% for SONDE and 48.37% for RUC, the probability of finding a cloud is 80%. Similarly, we could determine the RH thresholds at different probabilities (60%, 40%, and 20%) of finding a cloud as shown in Table 1.

By repeating above procedures for other RHs groups and plotting RH frequency distributions versus temperature, the frequency of cloud occurrence for a given RH and T is easily determined. The two-dimensional frequency distributions of cloud occurrence for both SONDE and RUC data are shown in Figure 8.

The RH threshold values used to make the clouds diagnoses with different probabilities for the RUC40 and SONDE are shown as red lines in Figures 8 and 9 for the comparison of SONDE (solid color lines) and RUC (dotted color lines). The drops in thresholds around 255 K are due to switch from RH with respect to water to RH with respect to ice. When $T < 245$ K, the RH thresholds do not vary much with temperature. At the same probability, the RH thresholds for SONDE are higher than ones for RUC except at warmer temperature ($T \geq 284$ K).

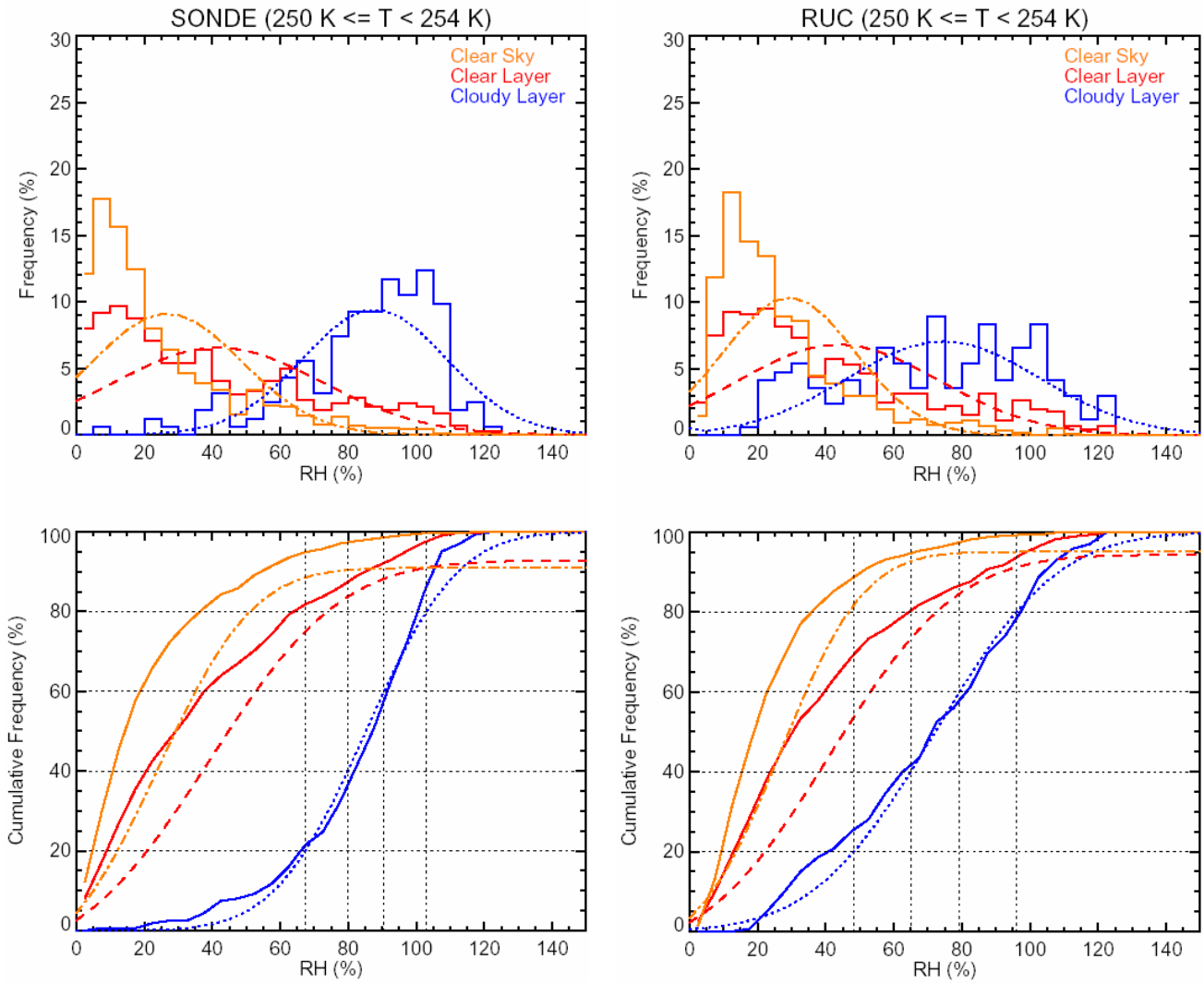


Figure 7. Frequency distributions of RH from all cloud layers where the ambient temperature is greater than 250 K and less than 254 K, for both SONDE and RUC.

Table 1. RH Threshold Values (%) for SONDE and RUC at Different Probabilities of Finding a Cloud when the Temperature is Between 250 K and 254 K.				
	P80	P60	P40	P20
SONDE	67.52	79.88	90.56	102.92
RUC	48.37	64.98	79.30	95.92

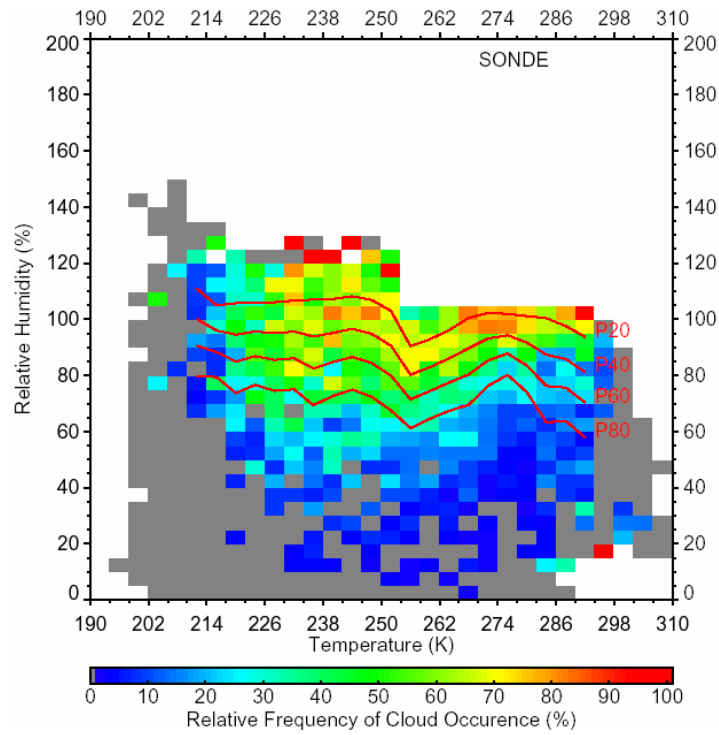


Figure 8. Two-dimensional frequency distribution of cloud occurrence for a given RH and T for both SONDE and RUC.

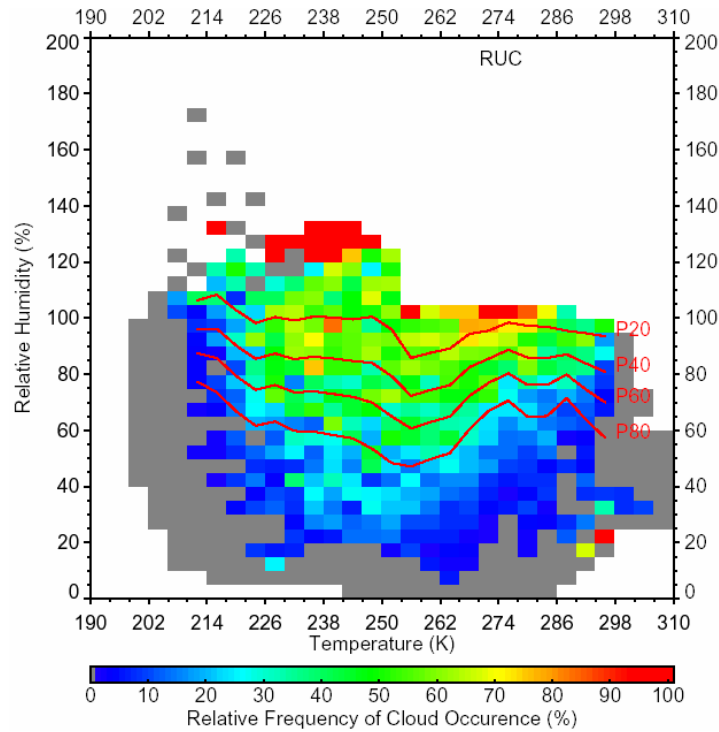


Figure 8. (contd).

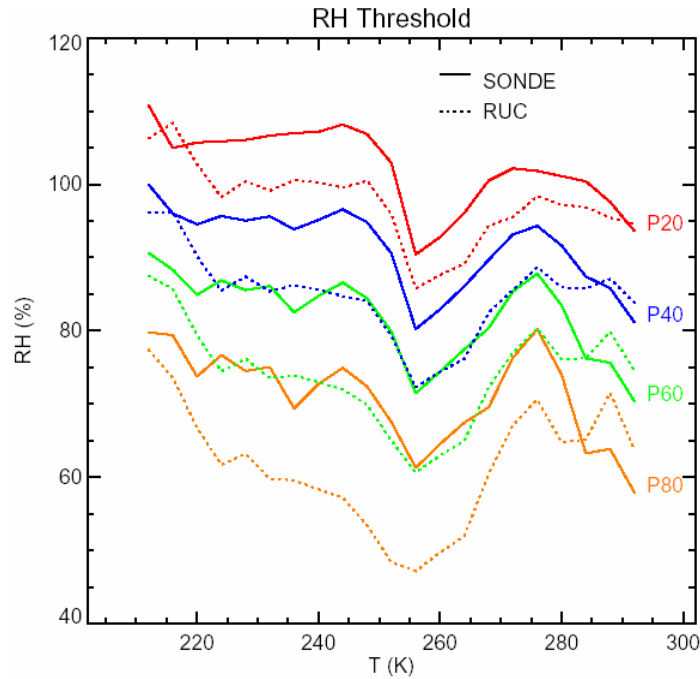


Figure 9. Comparisons of the RH threshold values from SONDE (solid lines) and RUC (dotted lines) at different probabilities of finding a cloud layer.

Validation of RH Thresholds

For a simple and quick check, the RH profiles from both SONDE and RUC are examined from the surface (1000 hPa) to 100 hPa to identify a layer in a profile as a clear or cloud layer. A layer which has RH equal to or exceeding the threshold values is identified as a cloud layer (Rcld). A layer having RH below the thresholds is determined to be a cloud-free layer (Rclr). The percentages of matched and mismatched layers in clear and cloud conditions for both SONDE and RUC for four probabilities of finding a cloud are shown in Table 2. Matched cases are those in which the layers are identified as either cloud layers or cloud-free layers by both ARSCL and RH-threshold method. Mismatched cases are those in which the layers identified as clear (cloud) layers by ARSCL are identified as cloud (clear) layers by RH-threshold method.

Table 2. The Percentage of Matched and Mismatched Layers In Clear and Cloud Conditions for Both SONDE and RUC.

	Aclr → Rclr		Acld → Rcld		Aclr → Rcld		Acld → Rclr	
	SONDE	RUC	SONDE	RUC	SONDE	RUC	SONDE	RUC
P80	85.74	79.19	82.73	79.27	14.26	20.81	17.27	20.73
P60	91.56	88.27	71.90	65.24	8.44	11.73	28.10	34.76
P40	95.36	93.74	53.90	49.62	4.64	6.26	46.10	50.38
P20	98.88	97.83	10.15	23.37	1.12	2.17	89.85	76.63

Note: Aclr – ARSCL clear layer; Acld - ARSCL cloud layer.
 Rclr – Clear layer determined by the RH threshold method; Rcld - cloudy layer determined by the RH threshold method.

If the probability of finding a cloud at a given RH and T is chosen, then the sounding can be used to specify cloudiness at a given level in the atmosphere. In other words, it can be used to construct a 3-D cloud dataset using an atmospheric profile from RUC or SONDE to help fill the volume underneath a given cloud observed from the satellite.

It is possible that no cloud exists when RH is high because other factors, such as vertical motion, also play a role in cloud formation.

Ice Supersaturation in the Upper Troposphere

Cloud-free air masses in a state of supersaturation with respect to ice are evident in the upper troposphere above the SCF site. Scatterplots of the RH in the upper troposphere (100 hPa – 400 hPa) from SONDE and RUC data are shown in Figure 10. As seen in the scatterplots RHI frequently exceeds 100%.

From Figures 4 and 10, it is clear that cloud-free ice supersaturated air exist in clear sky and cloud-free layers, though less than 10% (due to dry biases in the radiosonde data), as well as in cloudy layers. The opportunity to observe the cloud-free ice supersaturated layers in cloudy sky is greater than that in clear sky. This is supported by the study of Minnis et al. (2003) who found that on some days, contrails (ISSRs) predominately occur over clear areas and on other days, are seen more frequently over clouds.

Spichtinger et al. (2002, 2003) used data from the Microwave Limb Sounder (MLS) on board the Upper Atmospheric Research Satellite (UARS) and data from corrected RS80A operational radiosondes to study the humidity statistics inside and outside the ISSRs. They found that the probability of measuring a certain RHI, in the subsaturated and the supersaturated tropospheric ISSRs, respectively, decreases exponentially with the RH but with different slopes.

The distributions of the number of upper tropospheric layers having RH within a given 2% are shown in Figure 11. The separated exponential fits are adapted for RH above and below 100%. The slope of the exponential is steeper for RUC data than for SONDE data (shown in Table 2). A break of the exponential distribution occurs around $RH = 100\%$ for the tropospheric measurements, indicating the onset of ice formation. The exponential distribution of supersaturation for $RH > 100\%$ is characteristic of ISSRs. This exponential distribution is also found for $RH > 10\%$ (SONDE) and $RH > 20\%$ (RUC) in tropospheric subsaturated regions but with a flatter slope than in ISSRs (Table 3). The 50% probabilities for finding a cloud within a layer correspond to about 90 and 80% for the SONDE and RUC, respectively (Figure 9). Thus, the exponential fits might be more appropriately applied using SONDE and RUC data above 90 and 80%, respectively.

It is apparent that, in the upper troposphere, the current RUC modeled RH follows the simple statistical law, an exponential distribution, but with different slope than that found for the radiosonde measurements. Since water vapor is the most important greenhouse gas and because it might enhance the anthropogenic greenhouse effects via positive feedback mechanisms, it is important to represent its distribution correctly in atmospheric models. The determination of the RH distribution law makes it feasible to use simple tests to show whether the hydrological cycle in atmospheric models is represented in an adequate way or not.

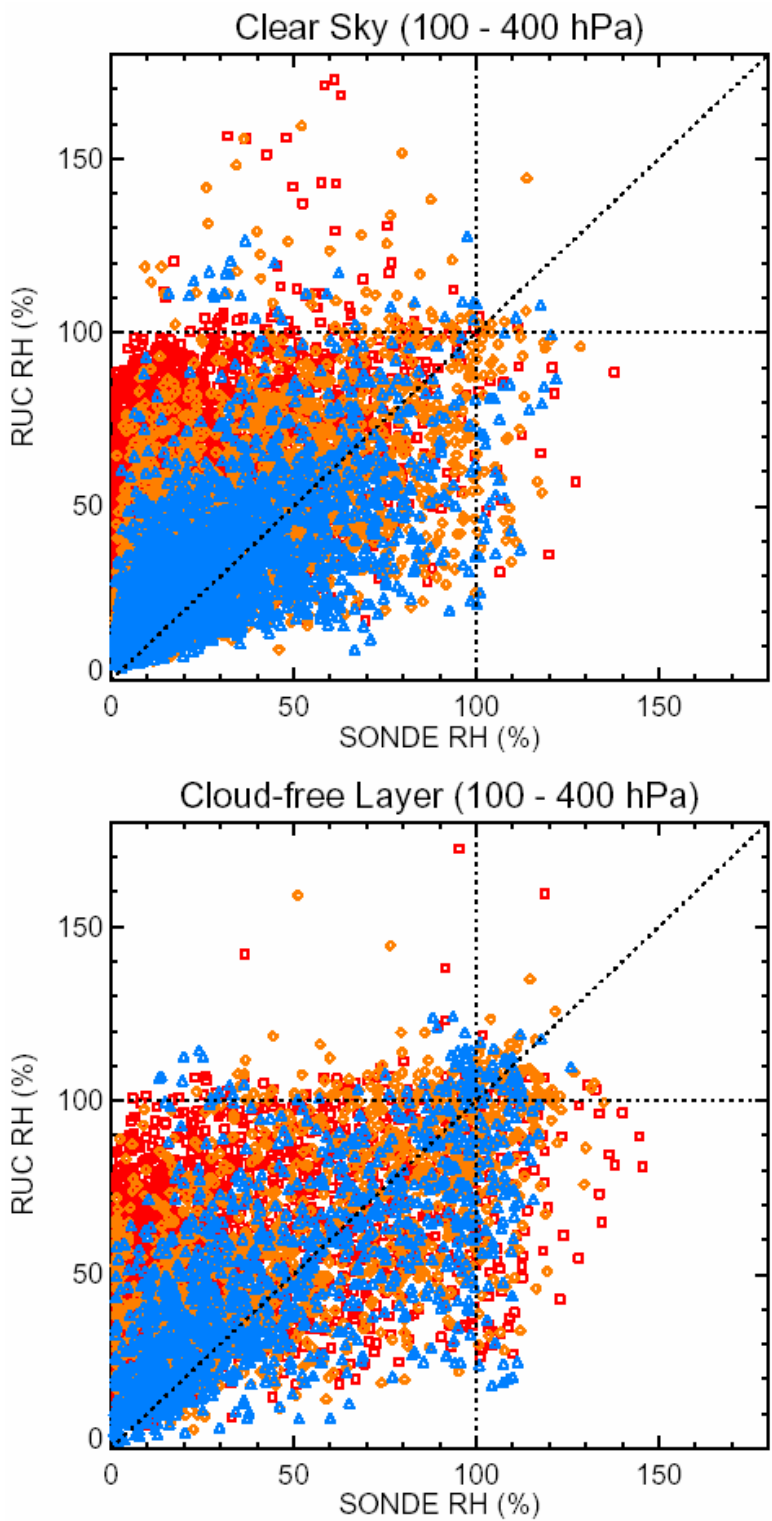


Figure 10. Scatterplots of the RH in the upper troposphere (100hPa to 400hPa) from SONDE (upper panel) and RUC (lower panel) in clear sky and cloud-free layers in cloud sky.

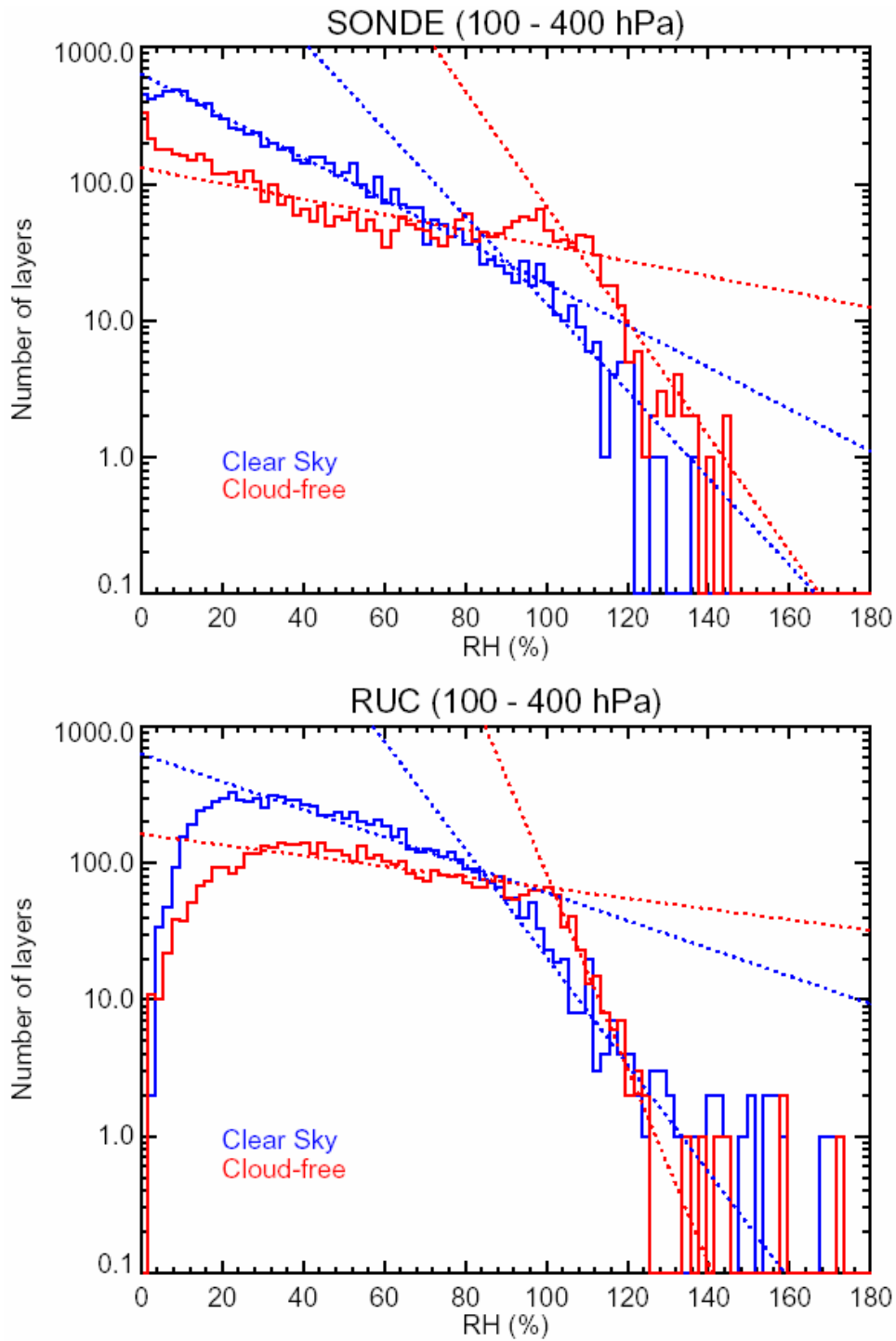


Figure 11. Statistical distributions (number of layers per 2% RH bin) of RH in clear-sky (blue) and cloud-free (red) troposphere for SONDE (upper panel) and RUC (lower panel). Several exponential fits (dotted lines) are presented.

Table 3. Slopes of Exponential Fits for SONDE and RUC.			
		SONDE	RUC
Supersaturated Region	Clear sky	0.074	0.091
	Cloud-free	0.097	0.164
Subsaturated Region	Clear sky	0.035	0.023
	Cloud-free	0.013	0.009

In future, the profiles from SONDE and RUC will be utilized to study the vertical extension of ice supersaturated air-masses and their relationship to the local tropopause.

Conclusions and Discussions

In this study, hourly RUC40 analyses from 1 March 2000 to 28 February 2001 were used to examine the differences between RH and temperature values from RUC reanalysis data and from radiosonde atmospheric profiles obtained at the ARM SCF. The results show that the temperature observations from the SONDE and RUC are highly correlated. The RHs are also well-correlated, but the SONDE values generally exceed those from RUC. Inside cloud layers, the RH from RUC is 2-14 % lower than the RH from SONDE for all RUC layers. Although the layer mean RH within clouds is much greater than the layer mean RH outside cloud or in the clear-sky, RH thresholds chosen as a function of temperature can more accurately diagnose cloud occurrence for either dataset. Overall, it was found that the 50% probability thresholds for diagnosing a cloud within a given upper tropospheric layer are roughly 90 and 80% for the Vaisala RS80-15LH radiosonde and RUC40 data, respectively. The probabilities of detecting clouds at a given RH and temperature suggest that an atmospheric profile from RUC or SONDE data can help fill the volume underneath a given cloud observed from the satellite when a 3-D cloud data set is being constructed. The relationship between cloudiness and RH and T found in this study may also be useful for improving cloud height and thickness retrievals from satellite by considering cloud vertical structure obtained from RH profiles in a given scene.

A major revision to the operational RUC model was implemented 17 April 2002. The RUC20 model with 20-km horizontal resolution replaced the RUC40 model. To improve quantitative precipitation forecasts, several changes in the way the model handles upper tropospheric moisture were made. The tropopause is more sharply defined, and most ice supersaturations for pressure levels less than 300 hPa are removed (Benjamin et al. 2004). These changes dry the upper troposphere relative to that in the RUC40. Thus, the RH thresholds used to make the cloud diagnoses for the RUC40 data need to be re-investigated and determined for RUC20.

Since the ARM program began in 1992, ARM used the Vaisala RS80-15LH radiosonde for all its sounding until April 2001. By comparing between total precipitable water vapor (PWV) obtained from radiosonde (Vaisala RS80-H) profiles and PWV retrieved from a collocated microwave radiometer (MWR), Turner et al. (2003) found that the RS80-H radiosonde has an approximate 5% dry bias compared to the MWR and there is a diurnal dependence in the magnitude of the bias, that is, daytime radiosondes are drier than nighttime radiosondes. Wang et al. (2002) developed a physically based correction, which is a function of age, RH, and ambient temperature and can be applied to the RS80 data to remove this dry bias. The correction brings the corrected radiosondes into nearly perfect agreement

with the microwave radiometer (in terms of total precipitable water vapor), and corrected nighttime radiosonde data show almost the exact same sensitivity to PWV as does the MWR.

Lebibe-scaled radiosondes (LSSONDE) products from the ARM have scaled the radiosonde's moisture profile to force agreement in PWV with the microwave MWR. This process improves the radiosonde profile by reducing sonde-to-sonde variability, removing dry bias and eliminating the diurnal feature in radiosondes.

New technology has greatly improved radiosonde performance at low temperature and water vapor concentrations. Since May 1, 2001, ARM began using the Vaisala RS90 radiosonde at the SGP site. RS90 radiosonde measures the atmospheric humidity with the new Vaisala H-Humicap sensor. There are two heated humidity sensors on RS90 operating in phases. While one sensor is used for measurement, the other sensor is heated to prevent ice formation.

Therefore, comparisons of the new RUC20 model analyses to data obtained from the new generation of radiosondes and contemporaneous ARSCL data are needed to determine the current relationships between atmospheric profiles and clouds. Further, the RH in the ice-supersaturated regions in the upper troposphere, from both model objective analyses and forecasts, and from radiosonde soundings, should be examined to determine if the simple statistical law still holds for the newer data.

Acknowledgments

This research was supported by the Office of Biological and Environmental Research of U.S. Department of Energy through the Interagency Agreements DE-AI02-97ER62341 and DE-AI02-02ER63319 as part of the Atmospheric Radiation Measurement Program.

Corresponding Author

H. Y.-H. Yi, y.yi@larc.nasa.gov

References

Benjamin, S. G., G. A. Grell, J.M. Brown, T. G. Smirnova, and R. Bleck, 2004a: Mesoscale weather prediction with the RUC hybrid isentropic/terrain-following coordinate model. *Mon. Wea. Rev.*, **132**:474-494.

Benjamin, S. G., and Coauthors, 2004b: An hourly assimilation/forecast cycle: The RUC. *Mon. Wea. Rev.*, **132**:495-518.

Clothiaux, E. E., M. A. Miller, R. C. Perez, D. D. Turner, K. P. Moran, B. E. Martner, T. P. Ackerman, G. G. Mace, R. T. Marchand, K. B. Widener, D. J. Rodriguez, T. Uttal, J. H. Mather, C. J. Flynn, K. L. Gaustad, and B. Ermold, 2001: The ARM Millimeter Wave Cloud Radars (MMCRs) and the Active Remote Sensing of Clouds (ARSCL) Value Added Product (VAP), March 4, 2001 (DOE Tech. Memo. ARM VAP-002.1).

Duda, D. P., P. Minnis, L. Nguyen, R. Palikonda, 2004: A case study of the development of contrail clusters over the Great Lakes. *J.A.S.*, **61**:1132-1146.

Gierens, K., U. Schumann, M. Helten, H.G.J. Smit, A. Marenco, 1999: A distribution law for relative humidity in the upper troposphere and lower stratosphere derived from three years of MOZAIC measurements. *Ann. Geophys.*, **17**:1218-1226.

Minnis, P., J. K. Ayers, M. L. Nordeen, and S. P. Weaver, 2003: Contrail Frequency over the United States from Surface Observations. *J. Climate*, **16**:3447-3462.

Minnis, P., J. K. Ayers, R. Palikonda, and D. N. Phan, 2004: Contrails, cirrus trends, and climate. *J. Climate*, **17**:1671-1685.

Ovarlez, J., J.-F. Gayet, K. Gierens, J. Strom, H. Ovarlez, F. Auriol, R. Busen, U. Schumann, 2002: Water vapor measurements inside cirrus clouds in northern and southern hemispheres during INCA. *Geophys. Res. Lett.*, **29**:1813.

Spichtinger, P., K. Gierens, W. Read, 2002: The statistical distribution law of relative humidity in the global tropopause region. *Meteorol. Z.*, **11**(2):83-88.

Spichtinger, P., K. Gierens, U. Leiterer, H. Dier, 2003: Ice supersaturation in the tropopause region over Lindenberg, Germany. *Meteorol. Z.*, **12**:143-156.

Turner, D., B. Lesht, A. Clough, J. Liljegren, H. Revercomb and D. Tobin, 2003: Dry Bias and Variability in Vaisala RS80-H Radiosondes: The ARM Experience. *J. of Atmos. and Oceanic Technol.*, **20**:117-132.

Wang, J., W. B. Rossow, 1995: Determination of Cloud Vertical Structure from Upper-Air Observations. *J. Appl. Meteor.*, **34**:2243-2258.

Wang, J., H. Cole, D. J. Carlson, E. R. Miller, K. Beierle, A. Paukkunen, and T. K. Laine, 2002: Corrections of humidity measurement errors from the Vaisala RS80 radiosonde Application to TOGA/COARE data. *J. Atmos. Oceanic Technol.*, **19**, 981– 1002.